Electronic Supplementary Material (ESI) for Inorganic Chemistry Frontiers.

Enhancement the properties of ZnAl-LDH for photocatalytic nitrogen reduction reaction by controlling anion intercalation

Senda Su, Xiaoman Li,* Mengyao Tan, Xu Zhang, Yingying Wang, Yanzhong Duan,, Juan Peng and Min Luo*

State Key Laboratory of High-efficiency Utilization of Coal and Green Chemical Engineering, School of Chemistry and Chemical Engineering, Ningxia University, Yinchuan, Ningxia 750021,
*Corresponding author: luominjy@nxu.edu.cn, lixm2017@nxu.edu.cn

Total number of pages: 19

Total number of figures: 16

Total number of tables: 1

Table of Contents

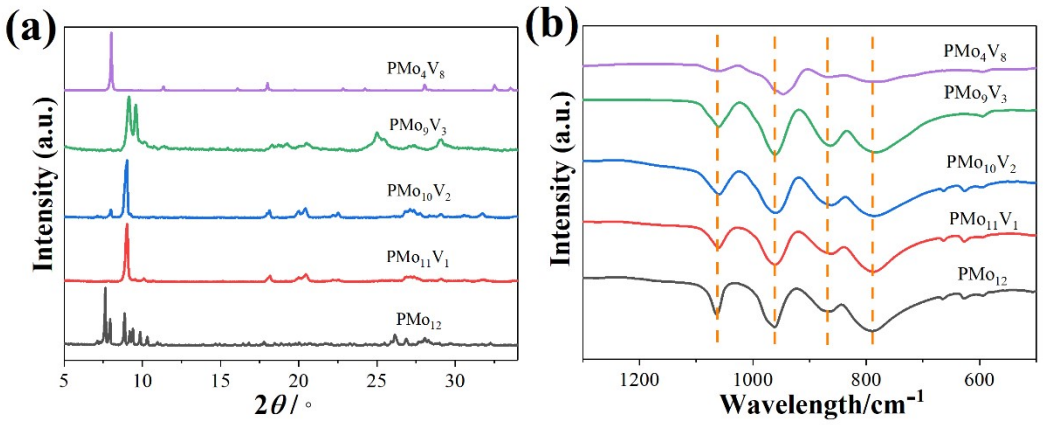

Figure S1. The XRD pattern (a) and FT-IR spectra (b) of $PMo_{12-X}V_X$ (X = 0, 1, 2, 3, 8).

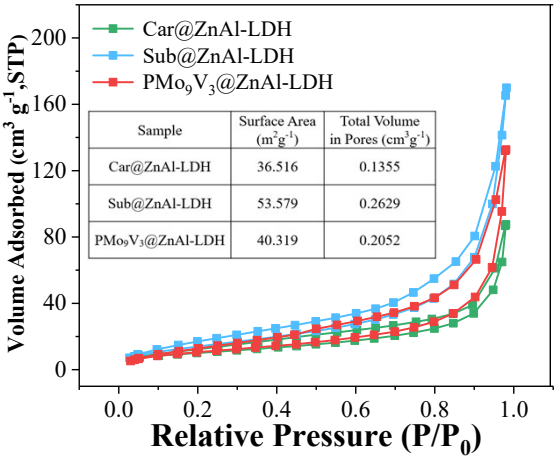

Sample	Surface Area (m^2g^{-1})	Total Volume in Pores (cm^3g^{-1})
Car@ZnAl-LDH	36.516	0.1355
Sub@ZnAl-LDH	53.579	0.2629
PMo_9V_3@ZnAl-LDH	40.319	0.2052

Figure S2. The N_2 adsorption–desorption isotherms and BET surface area of ZnAl-LDHs.

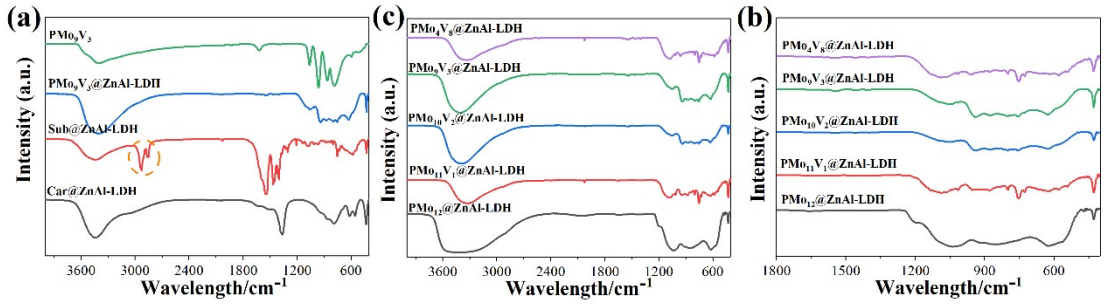

Figure S3. The FT-IR spectra of the ZnAl-LDHs at 400-4000 cm^{-1} (a and b), $PMo_{12-X}V_X$@ZnAl-LDH (X = 0, 1, 2, 3, 8) at 400-1800 cm^{-1}(c).

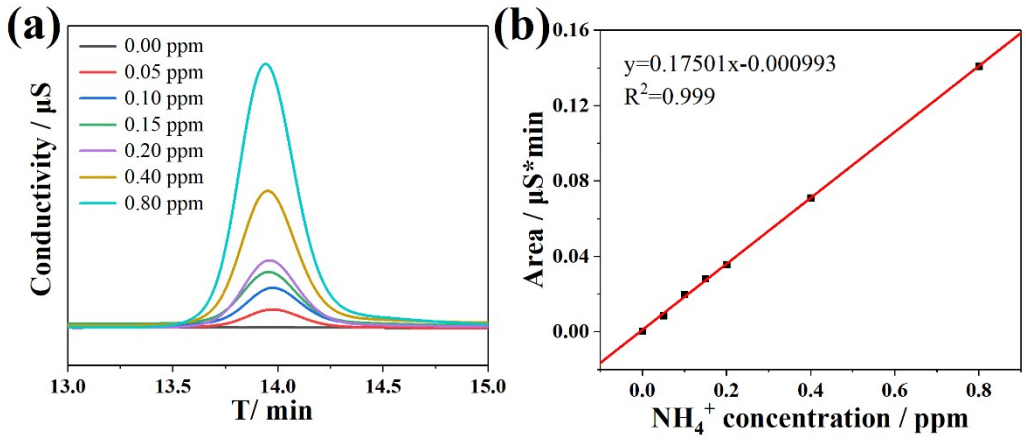

Figure S4. The NH_4^+ detection of standard spectra (a) and fitting curve (b) by ion chromatography.

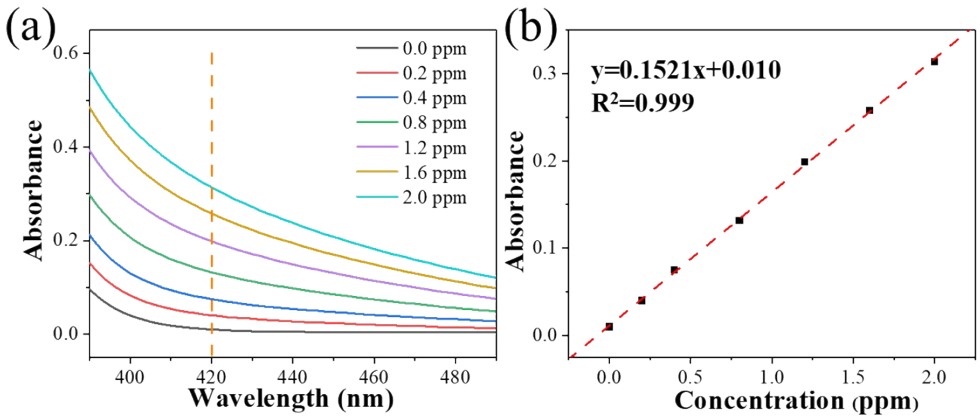

Figure S5. The NH_4^+ detection of UV-vis absorption spectra (a) and fitting curve (b).

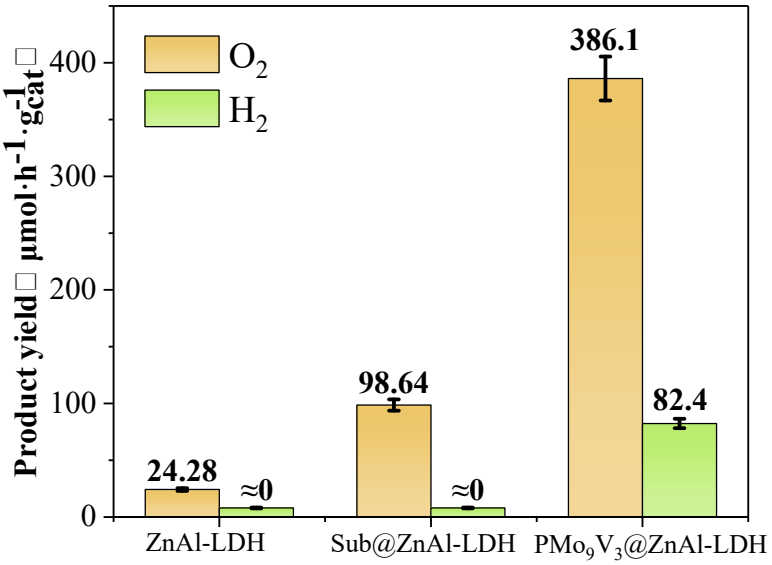

Figure S6. The gas phase products rate of the ZnAl-LDHs.

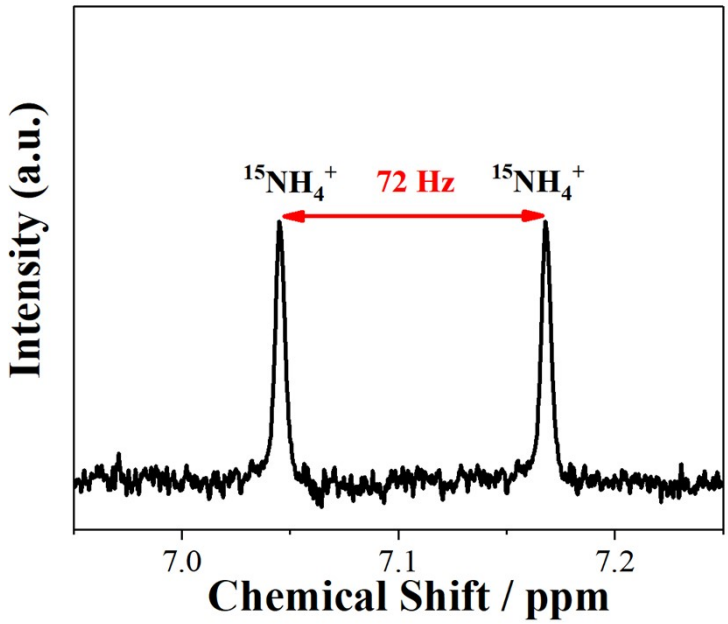

Figure S7. ^{1}H NMR spectra of the solution obtained after reaction using $^{15}N_2$ as the feeding gas on PMo_9V_3@ZnAl-LDH.

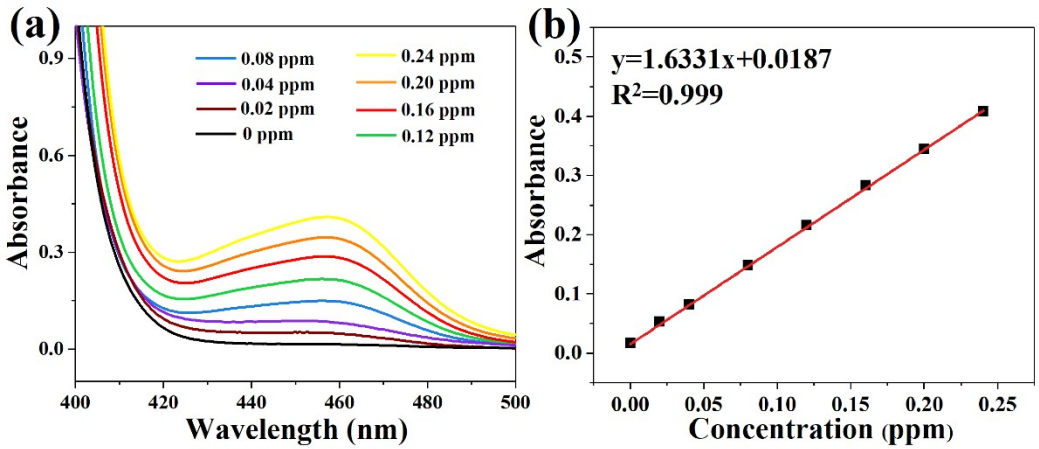

Figure S8. The N_2H_4 detection of UV-vis absorption spectra (a) and fitting curve (b).

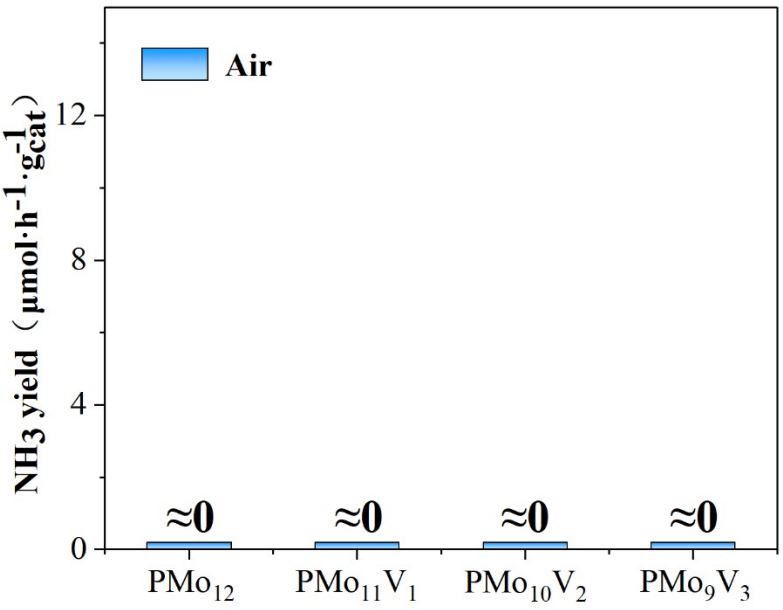

Figure S9. The NH_4^+ production rate of the PMoV in air.

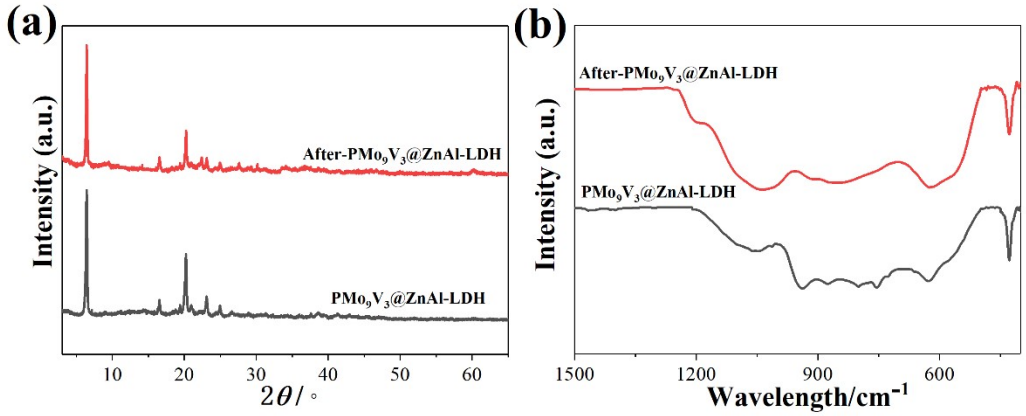

Figure S10. The XRD pattern (a) and FT-IR spectra (b) of PMo_9V_3@ZnAl-LDH before and after cycle reaction.

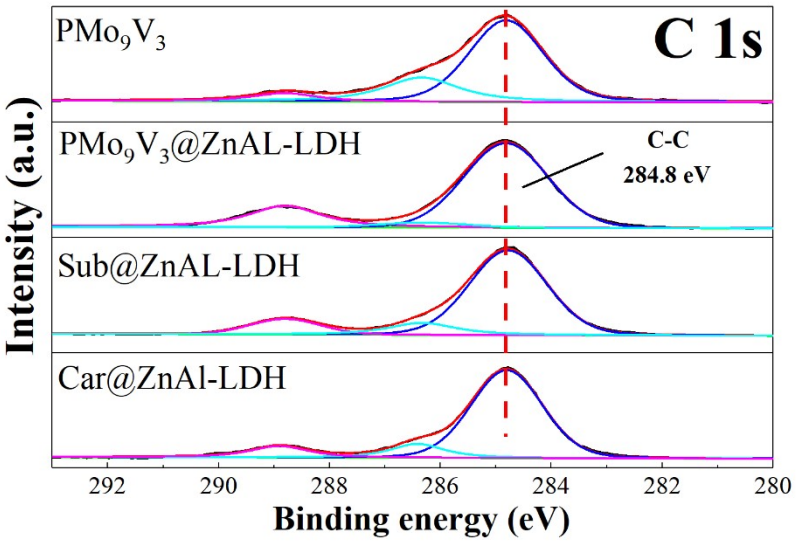

Figure S11. The C 1s XPS spectrum.

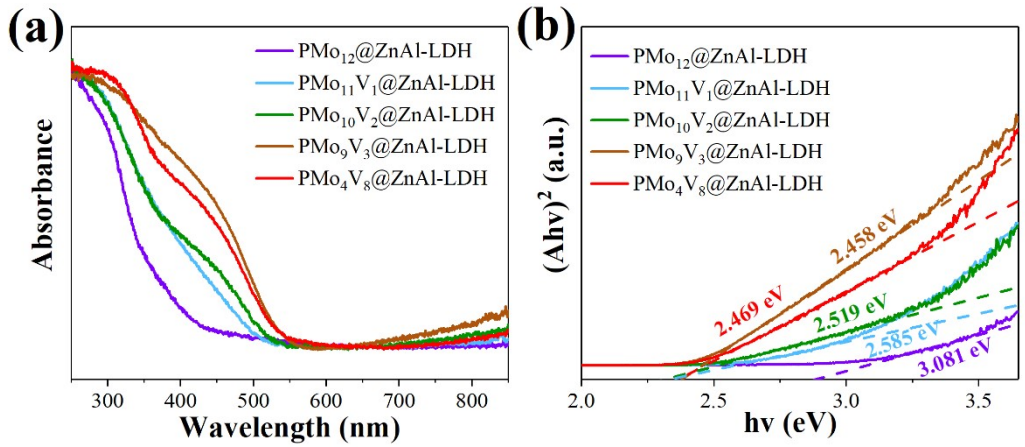

Figure S12. The UV-vis diffuse reflectance spectra (a) and Tauc plots (b) of $PMo_{12-X}V_X$@ZnAl-LDH (X = 0, 1, 2, 3, 8).

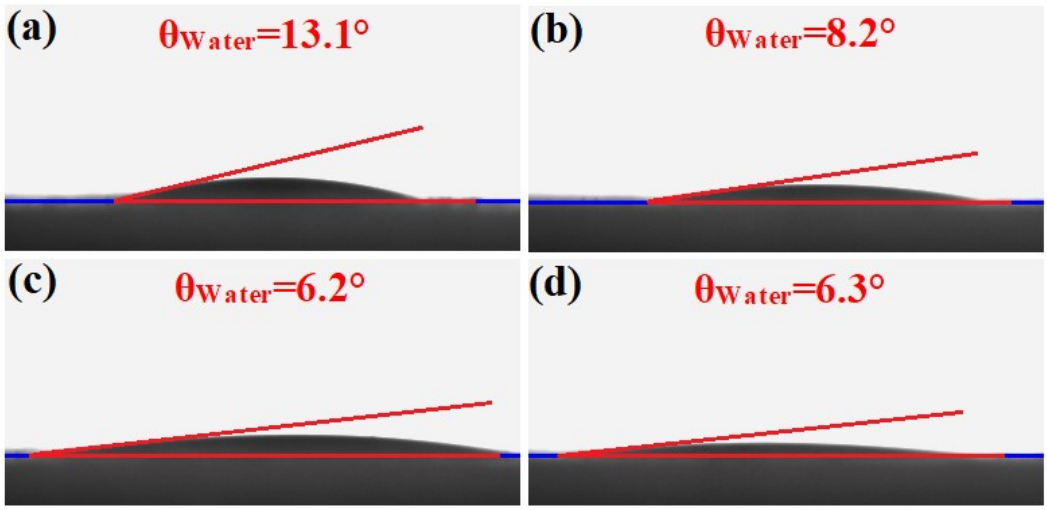

Figure S13. The contact angle images of $PMo_{12-X}V_X$@ZnAl-LDH (X = 1 (a), 2 (b), 3 (c), 8 (d)).

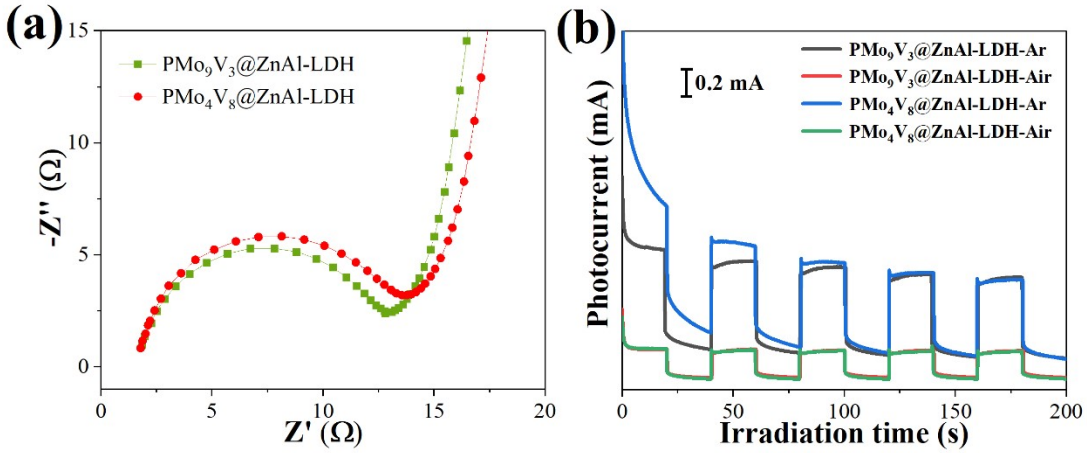

Figure S14. The EIS pattern (a) and photocurrent pattern (b) of $PMo_{12-X}V_X$@ZnAl-LDH (X = 3, 8).

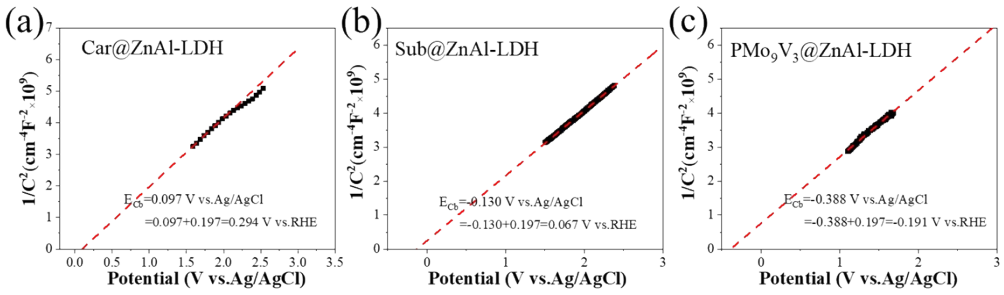

Figure S15. The Mott-Schottky curves of ZnAl-LDHs.

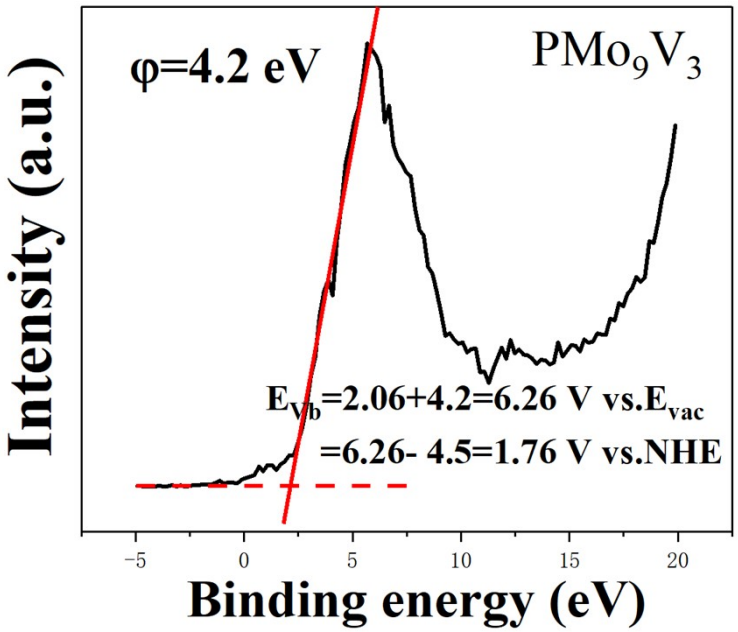

Figure S16. The VB XPS spectrum of PMo_9V_3.

Table S1. Photocatalytic nitrogen fixation performance of LDH-based materials.

Catalyst	Light source	Detection method	organic scavengers	NH_3 evolution rate/μmol h^{-1} g^{-1}_{cat}	Reference
NiV-LDH-11-AMO	Full spectrum	IC [a]	None	176	[1]
0.5%-CuZnAl-LDH	Full spectrum	IC [a]	None	110	[2]
ZnAl-LDH-NS	Full spectrum	NR [b]	None	15.28	[3]
ZnAl-LDH-1h(alkaline etching)	Full spectrum	IC [a]	None	25.76	[4]
Sub@ZnAl-LDH	Full spectrum	IC [a]	None	48.91	This work
PMo_9V_3@ ZnAl-LDH	Full spectrum	IC [a]	None	89.16	This work

[a] The detection method of ion chromatography.

[b] The detection method of Nessler's reagent.

[1] X. Liu, Y. Li, J. Zhang, J. Lu, Ultrathin Ni/V-layered double hydroxide nanosheets for efficient visible-light-driven photocatalytic nitrogen reduction to ammonia, Nano Research 14(10) (2021) 3372-3378.

[2] S. Zhang, Y. Zhao, R. Shi, C. Zhou, G.I.N. Waterhouse, L.-Z. Wu, C.-H. Tung, T. Zhang, Efficient Photocatalytic Nitrogen Fixation over Cu-delta(+)-Modified Defective ZnAl-Layered Double Hydroxide Nanosheets, Advanced Energy Materials 10(8) (2020).

[3] Y. Zhao, Y. Zhao, G.I.N. Waterhouse, L. Zheng, X. Cao, F. Teng, L.-Z. Wu, C.-H. Tung, D. O'Hare, T. Zhang, Layered-Double-Hydroxide Nanosheets as Efficient Visible-Light-Driven Photocatalysts for Dinitrogen Fixation, Advanced Materials 29(42) (2017).

[4] Y. Zhao, L. Zheng, R. Shi, S. Zhang, X. Bian, F. Wu, X. Cao, G.I.N. Waterhouse, T. Zhang, Alkali Etching of Layered Double Hydroxide Nanosheets for Enhanced Photocatalytic N_2 Reduction to NH_3, Advanced Energy Materials 10(34) (2020).